LIVE-LOAD DISTRIBUTION FACTORS IN PRESTRESSED CONCRETE GIRDER BRIDGES

By Paul J. Barr,[1] Marc O. Eberhard,[2] and John F. Stanton[3]

ABSTRACT: This paper presents an evaluation of flexural live-load distribution factors for a series of three-span prestressed concrete girder bridges. The response of one bridge, measured during a static live-load test, was used to evaluate the reliability of a finite-element model scheme. Twenty-four variations of this model were then used to evaluate the procedures for computing flexural live-load distribution factors that are embodied in three bridge design codes. The finite-element models were also used to investigate the effects that lifts, intermediate diaphragms, end diaphragms, continuity, skew angle, and load type have on distribution factors. For geometries similar to those considered in the development of the American Association of State Highway and Transportation Officials Load and Resistance Factor Design Specifications, the distribution factors computed with the finite-element models were within 6% of the code values. However, for the geometry of the bridge that was tested, the discrepancy was 28%. Lifts, end diaphragms, skew angle, and load type significantly decreased the distribution factors, while continuity and intermediate diaphragms had the least effect. If the bridge had been designed using the distribution factors calculated with the finite-element model rather than the code values, the required concrete release strength could have been reduced by 6.9 MPa (1,000 psi) or the live load could have been increased by 39%.

INTRODUCTION

Computing the response of a bridge to live loads is a complex task. The moment demand for a particular girder depends on the magnitude and location of the imposed loads and on the properties of the bridge. The design moment in the girder will vary with girder spacing, span, flexural stiffness, torsional stiffness, and on the properties of the deck and diaphragms. The presence of skew further complicates the task of estimating the design moment.

To simplify the design process, many bridge codes, such as the AASHTO Load and Resistance Factor Design (LRFD) Specifications (1998), the AASHTO Standard Specifications (1996), and the Ontario Highway Bridge Design Code (1992), treat the longitudinal and transverse effects of wheel loads as uncoupled phenomena. The design live-load moment caused by a truck (or lane of traffic) is first estimated by obtaining the maximum truck (or lane of traffic) moment on a single girder. A designer then obtains the design moments for each girder by multiplying the maximum single girder moment by a factor, which is usually referred to as the live-load distribution factor.

The goals of this paper are: (1) to evaluate the accuracy of a finite-element modeling strategy; (2) to evaluate code expressions for live-load distribution factors for prestressed concrete girder bridges; and (3) to evaluate the influence of lifts (the layer of concrete between the top of the girder and the bottom of the deck), intermediate diaphragms, end diaphragms, continuity, skew, and load type (truck or lane) on load distribution. The evaluation is limited to the geometry of a bridge on which the writers conducted a live-load test (Barr et al. 1999) and to 24 variations of that geometry.

LIVE-LOAD DISTRIBUTION FACTORS

The AASHTO Standard Specifications for Highway Bridges have contained live load distribution factors since 1931. The early values were based on the work done by Westergaard (1930) and Newmark (1948), but the factors were modified as new research results became available. For a bridge constructed with a concrete deck on prestressed concrete girders and carrying two or more lanes of traffic, the current distribution factor (AASHTO 1996) is $S/5.5$, where S is the girder spacing in feet. This factor, multiplied by the moment on a single girder, caused by one line of wheels, gives the girder design moment. The applicability of the procedures in the Standard Specifications is limited by the fact that they were developed considering only nonskewed, simply supported bridges. Piecemeal code changes over the years have also created inconsistencies (Zokaie et al. 1991a).

In 1994, AASHTO adopted the LRFD Bridge Design Specifications (AASHTO 1994) as an alternative to the Standard Specifications. The LRFD expressions for live-load distribution are based on the results of a parameter study by Zokaie et al. (1991b), which considered variations in girder spacing, girder stiffness, span length, skew, and slab stiffness. The resulting LFRD expressions account for many parameters that were neglected previously, including skew. According to Zokaie et al., the LRFD code distribution factors lie within 5% of the distribution factors calculated with detailed finite-element models.

The finite-element models used to develop the AASHTO LRFD (1994) code equations were detailed, but the models did not include all of the components of a typical bridge. For example, Zokaie et al. considered the effects of diaphragms in a pilot study but not in the main parameter study. In addition, the factor that Zokaie et al. proposed to account for girder continuity was not included in the LRFD Specifications. Consequently, the LRFD code expressions are based on the results of analyses for HS20 loading of simply supported bridges without lifts, intermediate diaphragms, or end diaphragms.

The AASHTO LRFD equations for the distribution factors are more accurate than those provided in the Standard Specifications (Mabsout et al. 1997). However, Chen and Aswad (1996) found that the LRFD code distribution factors can be uneconomically conservative for bridges with large span-to-depth ratios. Based on the results of finite-element analysis, Chen and Aswad found that this conservatism could be as much as 23% for interior beams and 12% for exterior beams. A reduction in the conservatism of the code would lead to more economical bridge designs.

Further research was needed to evaluate the accuracy of the code live-load distribution factors and to quantify the effects

[1]Grad. Student, Univ. of Washington, Seattle, WA 98195.
[2]Assoc. Prof., Univ. of Washington, Seattle, WA 98195.
[3]Prof., Univ. of Washington, Seattle, WA 98195.

Note. Discussion open until March 1, 2002. To extend the closing date one month, a written request must be filed with the ASCE Manager of Journals. The manuscript for this paper was submitted for review and possible publication on November 29, 1999; revised June 2, 2000. This paper is part of the ***Journal of Bridge Engineering***, Vol. 6, No. 5, September/October, 2001. ©ASCE, ISSN 1084-0702/01/0005-0298–0306/ $8.00 + $.50 per page. Paper No. 22093.

of parameters not considered in the codes or most previous analyses.

SR18/SR516 BRIDGE

As part of a study of high-performance concrete in prestressed concrete girders, the Washington Department of Transportation (WSDOT) designed a bridge to carry the eastbound lanes of State Route 18 (SR 18) over SR 516. The writers performed a live-load test on the bridge as part of the study. The SR18/SR516 bridge has three spans with lengths of 24.4, 41.7, and 24.4 m (80, 137, and 80 ft) (Fig. 1). The skew angle was 40°. The girders were designed to have a concrete strength of 51 MPa (7,400 psi) at release and 68.9 MPa (10,000 psi) at 56 days (Barr et al. 1998).

Fig. 1 shows a plan of the bridge. Each of the five girder lines is denoted with a letter (A–E), and each span is identified with a number (1–3). At piers 1 and 4, the girders were supported on elastomeric bearings. At piers 2 and 3, the girders rested on grout pads.

The Washington State W74MG cross section was used for all girders (Fig. 2). In the field, the girders were made composite with a 190 mm (7.5 in.) deck slab. The girders were made continuous over piers 2 and 3 by placing substantial top reinforcement in the deck and casting the pier diaphragms around reinforcement projecting from the girders. Fig. 3 shows a cross section of the bridge at midspan. Directly above the girder, the deck thickness was increased to 285 mm (11.25 in.). The extra thickness of 95 mm (3.75 in.), referred to as the lift, was intended to compensate for camber differences among the girders. At the time of testing, the traffic barriers had not yet been placed on the bridge.

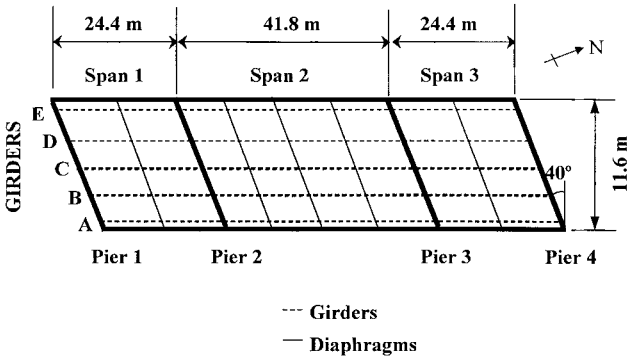

FIG. 1. Bridge Layout

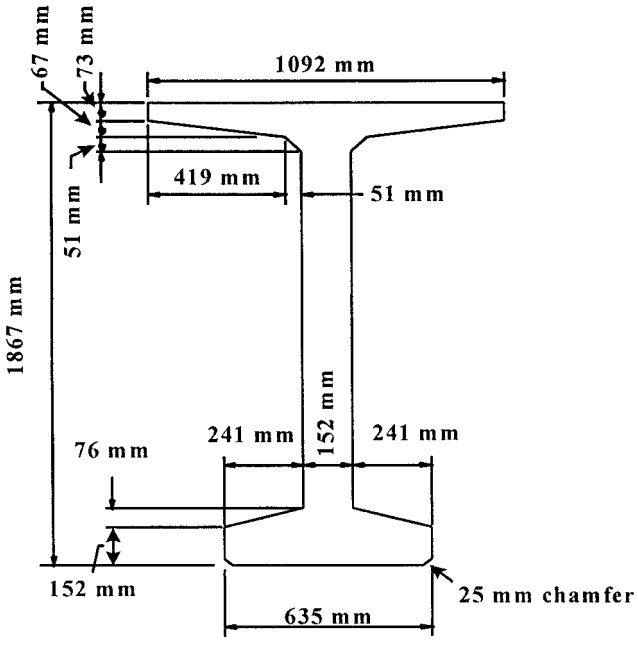

FIG. 2. W74MG Cross Section

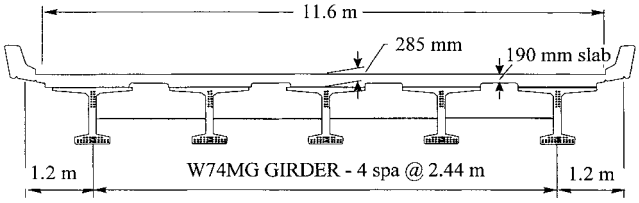

FIG. 3. Bridge Cross-Section at Midspan

Intermediate diaphragrms were placed at midspan for spans 1 and 3 and at quarter spans long Span 2. They extended 1,090 mm (43 in.) below the deck slab and were connected through the web of each girder with a #8 bar at the top of the diaphragms and a #9 bar at the bottom.

DESCRIPTION OF LIVE-LOAD TEST

A two-axle dump truck that weighed 158 kN (35.6 kips) was used to apply loads to the bridge (Barr et al. 1999). Although the truck was not as heavy or as long as an AASHTO HS20 design truck [320 kN (72 kips)], it was the largest available at the time of the test. The response of the bridge to this loading was used to evaluate the accuracy of a finite-element model. The analytical model was then loaded with AASHTO trucks to compute the live-load distribution factors. The dump truck had front and back axle loads of 49.4 kN (11.1 kips) and 109 kN (24.5 kips), separated longitudinally by a distance of 4.42 m (14.5 ft). The transverse center-to-center distance between wheels was 1.83 m (6.0 ft).

The truck was placed at various locations in order to determine the bridge's response to live loads. For each girder line, the truck traveled from span 1 to span 3, stopping at each selected location. Then, the truck turned around and returned along the same line, stopping at fewer locations. The truck followed this same pattern for all five girder lines. Fig. 4 shows a plan view of the bridge. At each single arrow location, a reading was taken with the truck oriented in the direction of the arrow. Where two arrows point in opposite directions, a reading was taken with the truck oriented in both directions.

Before moving the truck along a girder line, initial strain and temperature readings were taken with the truck off the bridge. After the strain readings were measured for a particular girder line, a second zero reading was taken. Random variations were shown independently to cause strains of less than one microstrain. Therefore, changes in zero readings were assumed to result from thermal effects.

In span 2, 40 vibrating wire strain gauges (VWSGs) were embedded in the W74MG bridge girders to monitor longitudinal strains (Barr et al. 1998). The gauges were installed at midspan and at 5 ft from the ends. The moments were calculated from differences in the strain readings caused by loading the bridge. In making this calculation, the composite cross section was assumed to include the girder, lift, and slab. The elastic moduli were derived from cylinder tests on the girder and deck concrete. Individual zero (unloaded) readings for every load location were found by linearly interpolating on temperature (based on the gauge temperature at the time of loading) between the initial and final zero reading for that girder line.

The measured moment was calculated from the recorded strain values. Girders A and B were heavily instrumented, and each contained two gauges that were installed at the same height in the bottom flange. In girders C and E, only one bottom gauge was available.

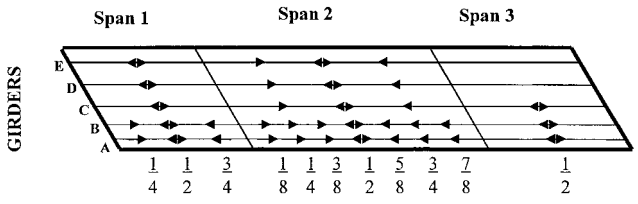

FIG. 4. Truck Location for Readings

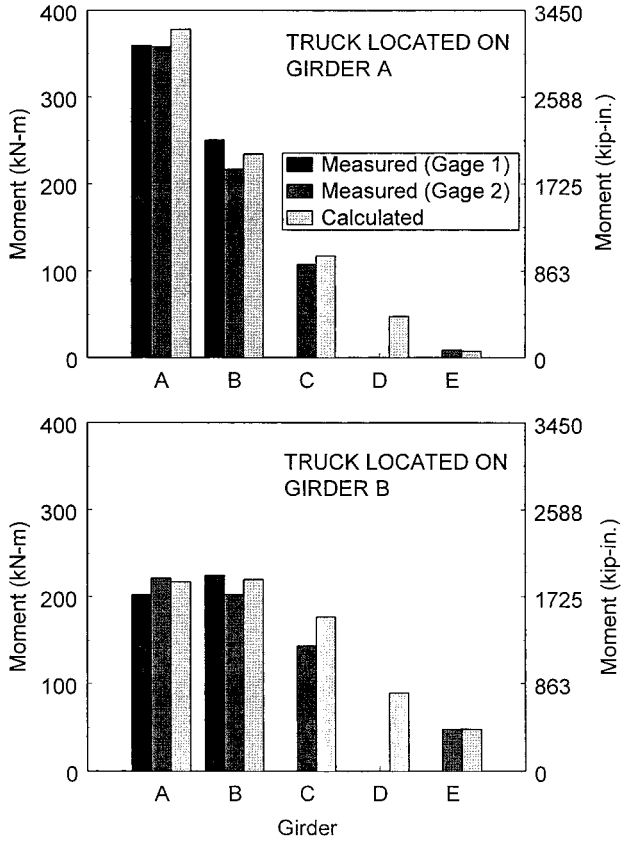

FIG. 5. Measured and Calculated Midspan Moments Due to Midspan Loading

Fig. 5 presents measured midspan moments for a truck located at midspan of girders A and B. For a truck located near the edge of the deck (girder A), the moment was largest in the edge girder and diminished progressively in the more distant girders. For a truck located on the first interior girder (girder B), the moments were nearly equal in the edge girder and the first interior girder.

The maximum moment for girders A, C, and E occurred when the truck was placed directly over the girder in question. The largest moment in B occurred when the truck was placed directly over girder A.

FINITE-ELEMENT MODEL

A finite-element model of the SR18/SR516 overcrossing was developed to evaluate the live-load distribution procedures recommended by AASHTO. The model had to be sufficiently accurate to reproduce the behavior observed during the live-load test and sufficiently versatile to permit modeling of all the bridge components. It also had to be able to simulate truck loading of bridges with a variety of loading conditions and skew angles. This requirement dictated the need for a fine element mesh in the deck, so that the nodes would be near the truck wheels, regardless of the skew angle. A node spacing of approximately 2 ft transversely, to fit the 8 ft girder spacing, and 1 ft longitudinally was eventually chosen. This mesh had

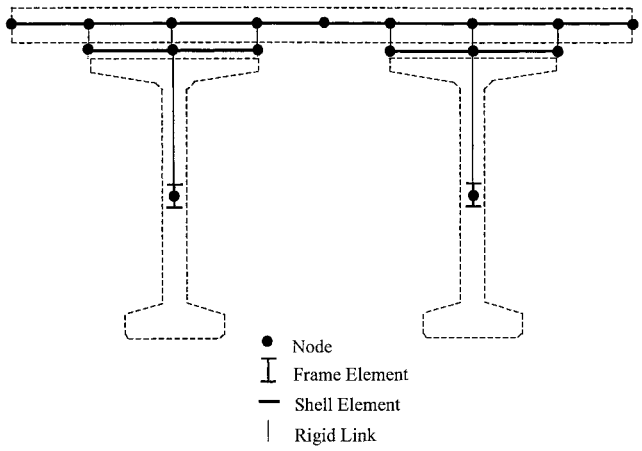

FIG. 6. Cross Section of Finite-Element Model of Two Girders

approximately 6,000 nodes in the plane of the deck. It was finer than those used in previous studies (e.g., Chen and Aswad 1996; Mabsout et al. 1997).

Many previous studies have shown that, to obtain accurate results, the flexural and torsional stiffnesses of the girders must be modeled correctly (Stanton and Mattock 1986; Chen and Aswad 1996), and the vertical placement of the members in the model should reflect that of the prototype (Nutt et al. 1987). After a number of trials, the arrangement of nodes and elements shown in Fig. 6 was selected. It offered the following features: (1) the vertical location of the deck, lift, and girder elements reflected accurately the locations of those members in the bridge; (2) the flexural and torsional properties of the precast girders could be lumped in the frame elements that were placed at the center of gravity of the girders; (3) bending moments in the composite girders could be extracted from the output easily; and (4) the number of nodes (12,000) was small enough to offer a tractable solution.

Both the intermediate diaphragms and the pier diaphragms were modeled using shell elements. The pier diaphragms were made to act compositely with the pier caps through the use of rigid constraints.

The finite-element model included columns and a pier cap beam at the intermediate piers. The columns and pier cap beams were modeled with 1 ft long frame elements. At each abutment, the elastomeric bearings in the bridge were represented in the analytical model by releasing horizontal displacements. The values of Young's modulus, E, for the various elements in the finite-element model were measured from material tests (Barr et al., 1998). Poisson's ratio, ν, was assumed to be 0.20. This modeling strategy was implemented using SAP2000 (*SAP2000* 1997).

EVALUATION OF ANALYTICAL MODEL

The response of the finite-element model of the SR18/SR516 overcrossing was analyzed for the truck locations shown in Fig. 4. Fig. 5 compares the calculated and measured midspan moments for all four instrumented girders when the truck was placed at the midspan of girders A and B. Here, ''calculated'' moments are those computed from the finite-element model and ''measured'' moments are those derived from the measured strains. For girders A and B, the magnitude of the difference between the measured and calculated moments is about the same magnitude as the difference between the two measured moments derived from the individual gauge readings.

Fig. 7 shows a comparison between calculated and measured moments at midspan due to placement of a single truck at midspan. Five load cases, each represented by a different

symbol, are included. Each load case consists of a truck placed over a girder and has four associated response locations (girders A, B, C, and E). The straight line represents a perfect correlation between the calculated and the measured moments.

The calculated moments were close to the measured ones. The calculated moment was slightly larger than the measured moment in almost all cases, but for the maximum moment in each girder, the largest discrepancy was less than 6%.

The circle and inverted triangle in the top right corner of Fig. 7 each represent the midspan response of an exterior girder (A and E) due to a load at midspan of the respective girder. These responses are much larger than the responses of the other girders and control the girder design.

The midspan measured and calculated responses were also compared as the truck moved along each girder line. Fig. 8 shows the influence lines for midspan moment in span 2 for girders A and B. In girder line A, the measured midspan moment was smaller than the calculated moment when the truck

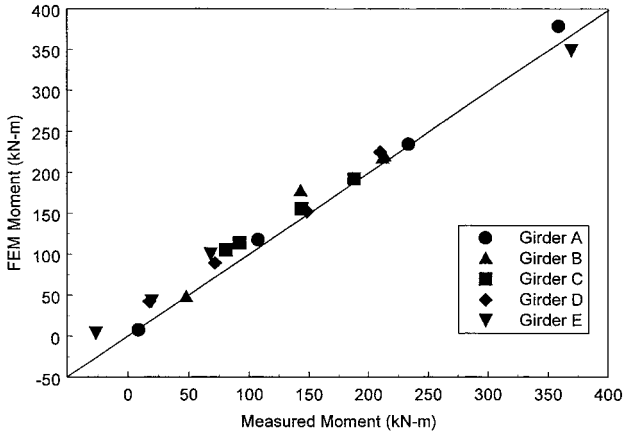

FIG. 7. Comparison of Measured and Calculated Midspan Moments

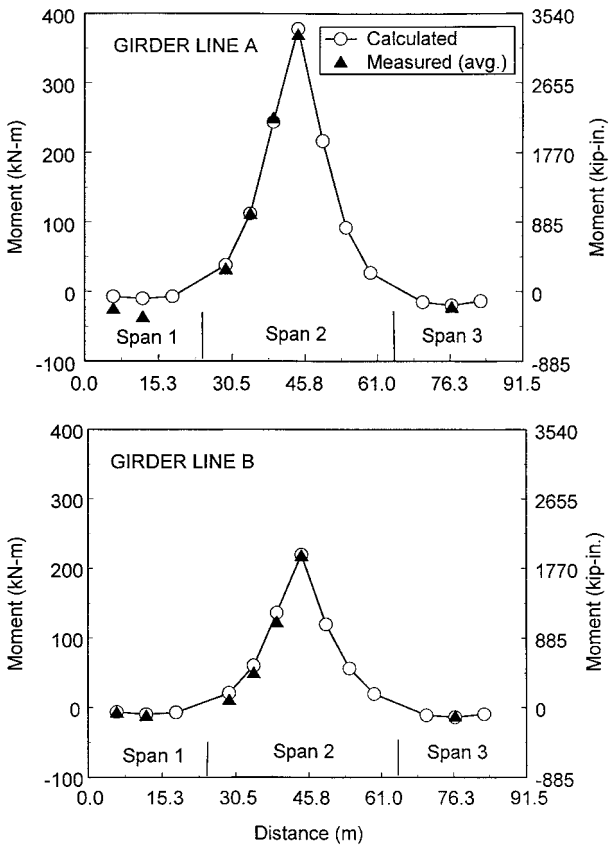

FIG. 8. Influence Lines for Midspan Moment

was located in span 1, but the moments were nearly identical when the truck was located in spans 2 and 3. Measured and calculated moments for girder line B were nearly identical, regardless of the truck location.

The agreement between calculated and measured moments, for both transverse and longitudinal profiles, verified that the finite-element model reflected well the behavior of the prototype bridge.

VARIATIONS OF FINITE-ELEMENT MODEL

A series of progressively more detailed models of the SR18/SR516 overcrossing was developed. The first model (model 1) was a simply supported, single-span model of span 2 with only the deck and girders modeled. This model did not account for lifts, intermediate diaphragms, end diaphragms, or span continuity. This model is similar to that used in developing the AASHTO LRFD Specifications (1998) (Zokaie 1991b).

Other models were developed to study the influence that the lifts, intermediate diaphragms, end diaphragms, and continuity had on the live-load distribution factors. By adding one member type at a time, its influence on the distribution factors could be isolated. The second model (model 2) was the same as model 1, but lifts were included between the girders and deck. In model 3, intermediate diaphragms were added, and in model 4 end diaphragms were added. Model 5 was the same as model 4, but spans 1 and 3 were added and the three spans were made continuous. Model 5 best represents the SR18/SR516 overcrossing and was the one used for comparison with the measured results (Figs. 5, 7, and 8). In addition, the skew angle of each model was varied between 0 and 60° to evaluate the effect of skew.

EVALUATION OF CODE LIVE-LOAD DISTRIBUTION FACTORS

To evaluate the various code live-load distribution factors, models 1 and 5 were compared with the AASHTO LRFD Specifications (1998), AASHTO Standard Specifications (1996), and the OHBDC (1992).

Calculation of Finite-Element Model Distribution Factors

To compute the distribution factors for the finite-element models, the writers considered truck load cases that were similar to those analyzed by Zokaie et al. (1991b). For each model, the longitudinal position of the AASHTO truck was established by finding the location where an AASHTO truck produced the maximum midspan moment on an isolated beam of the same span. The AASHTO trucks were then placed longitudinally in the same position on the finite-element model.

The AASHTO trucks were positioned transversely by dividing the bridge into as many 12 ft wide lanes as possible (three) and placing an AASHTO truck, with a 6 ft wheel spacing, in each lane. For each lane pattern, a series of transverse truck locations within each lane was then considered. Wheels of adjacent trucks were never closer than 4 ft, and the curb edge distance was never less than 2 ft. Lanes were also systematically moved, which created a total of 35 load cases.

For each model and load case, the midspan moment in each girder was recorded. These moments were used to calculate the distribution factors as follows. Multilane reduction factors of 1.0 and 0.85 were applied to all the moments calculated with a two- and three-lane load condition, respectively (Zokaie 2000). Then, the maximum moment from all 35-load cases was obtained for each of the five girders. From the maximum moments for each girder, the maximum exterior and interior moments were selected. Finally, the distribution factors for the

interior and exterior girders were found by dividing the maximum interior and exterior girder moments by the static moment calculated for a single AASHTO truck placed on the isolated beam. For models 1–4, the isolated beam was simply supported. For model 5, the isolated beam was continuous over the three spans. In all cases, the finite-element model results were computed for skew angles ranging from 0 to 60°.

Calculation of Code Distribution Factors

The live-load distribution factors investigated in this study were calculated using the methods given in the AASHTO LRFD Specifications (1998), AASHTO Standard Specifications (1996), and the Ontario Highway Bridge Design Code (OHBDC) (1992).

The live load distribution factors for the AASHTO LRFD Specifications were calculated as recommended, including the correction factors for skew. The formulas already include multilane reduction factors (Zokaie et al. 1991b).

The AASHTO Standard Specifications do not distinguish between exterior and interior girders, nor do they account for the effect of skew. These specifications require the use of a multilane reduction factor of 0.9 for three-lane bridges. This factor was applied to the distribution factors from the Standard Specifications when comparing them with the results of the finite-element distribution factors in this study. Also, because the Standard Specifications are expressed in terms of wheel loads (half of the AASHTO axle loads), the distribution factors from the Standard Specifications were divided by two in order to compare them directly with the AASHTO LRFD Specifications and finite-element distribution factors.

The Ontario Highway Bridge Design Code (1992) load distribution factors apply only for skew angles up to 20°. In addition, the initial load distribution factor (*D*) already includes a multilane reduction factor. Like the Standard Specifications, the OHBDC uses wheel loads, so its distribution factors were also divided by two for the comparison.

Fig. 9 shows the truck live load distribution factors from the three codes and finite-element models 1 and 5. The distribution factors are plotted for skew angles ranging from 0 to 60°.

The distribution factors from model 1 are on average 6% lower than those from the AASHTO LRFD Specifications. This difference is close to the 5% difference reported by Zokaie (1991a). The consistencies between the two studies should be expected, because the parameter study on which the code was based used a single-span model similar to model 1. Model 5 represents most closely the details of the SR18/SR516 overcrossing. On average, the LRFD code distribution factors were 28% higher than those obtained with model 5.

Similarly, the distribution factors calculated with the AASHTO Standard Specifications (1996) are closer to those calculated from model 1 than from model 5. A key shortcoming of the Standard Specifications is that they do not take into account the effect of skew.

The distribution factors from the OHBDC are very close to those of model 5 for small skew angles, but they are unconservative for model 1.

EFFECT OF PARAMETER VARIATIONS ON DISTRIBUTION FACTORS

To investigate the significant differences between the distribution factors for models 1 and 5, the effects of lifts, intermediate diaphragms, end diaphragms, and continuity were evaluated.

Effect of Lifts

The lift slightly increases the composite girder stiffness. More importantly, because the top flange width of the W74MG is a significant fraction of the girder spacing, the addition of a 95 mm (3.75 in.) lift increases the effective thickness of the deck and thus the transverse bending stiffness. This change leads to an increase in the ratio of transverse to longitudinal stiffness, which in turn implies a more uniform distribution of girder moments and a lower live-load distribution factor.

The difference between models 1 and 2 was the presence of a lift between the top of the girder and the bottom of the deck. Fig. 10 compares the distribution factors for models 1 and 2 as the skew varies. The difference between the distribution factors from models 1 and 2 increased slightly with skew. On average, the addition of the lift reduced the distribution factors by 17% for the exterior girders and by 11% for the interior girders. In contrast, if the lift is added to the girder cross section, the LRFD distribution factors increase by 1%.

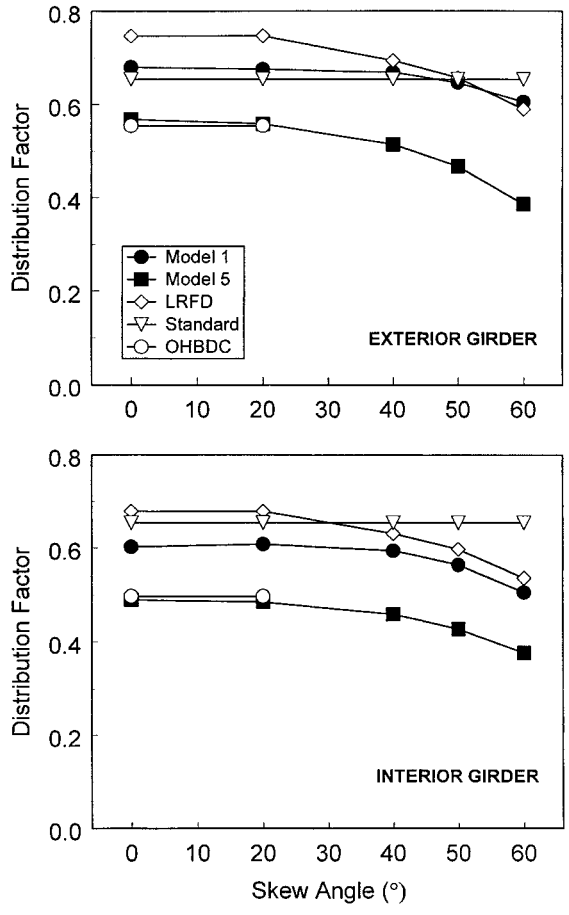

FIG. 9. Comparison of Live-Load Distribution Factors with Codes

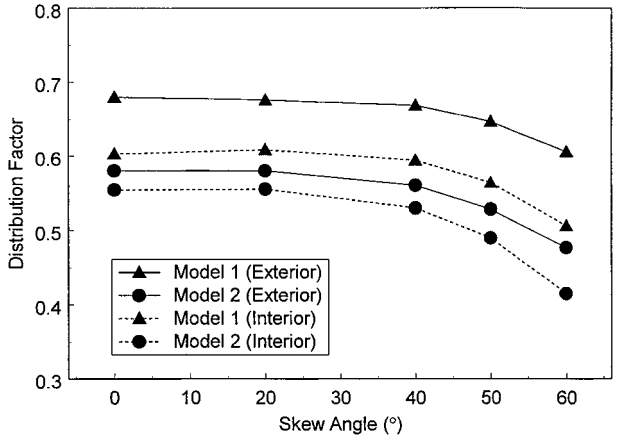

FIG. 10. Effects of Lifts

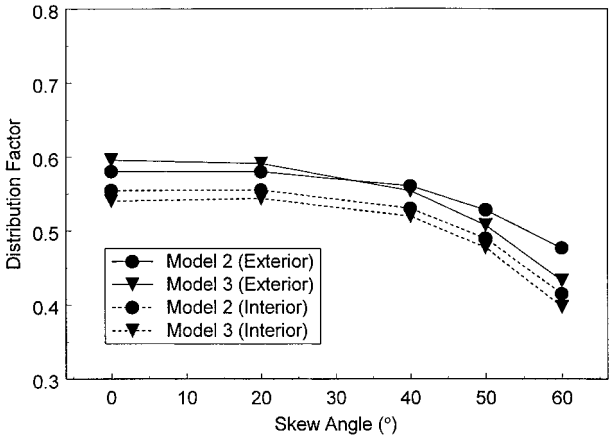

FIG. 11. Effects of Intermediate Diaphragms

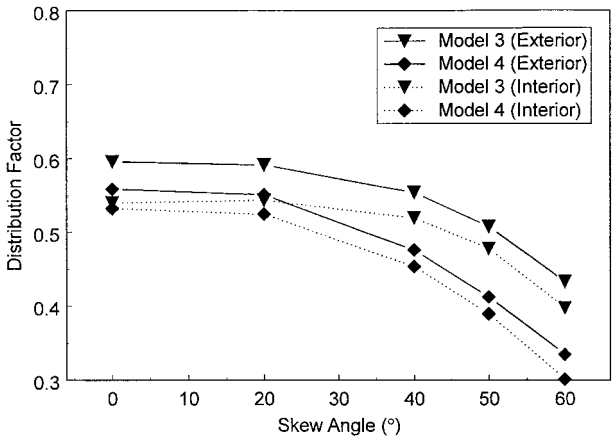

FIG. 12. Effects of End Diaphragms

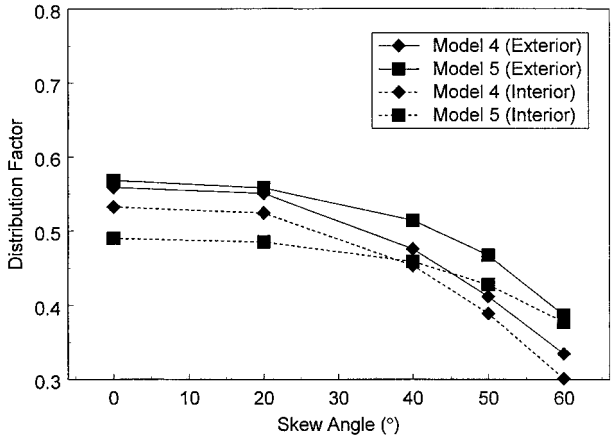

FIG. 13. Effects of Continuity

Effect of Intermediate Diaphragms

The only difference between models 2 and 3 was the addition of intermediate diaphragms in model 3. Live-load distribution factors for the two models are shown in Fig. 11. For both interior and exterior girders, the addition of intermediate diaphragms had less impact on the live-load distribution factors than did any other variable investigated. This finding is in agreement with the conclusions of Sithichaikasem and Gamble (1972).

For the exterior girders, the intermediate diaphragms slightly increased the live-load distribution factor at low skew angles. At high skew angles ($\geq$30°) the diaphragms were slightly beneficial. This behavior has also been observed by others (Sithichaikasem and Gamble 1973; Stanton and Mattock 1986).

Effect of End Diaphragms

End diaphragms influence the midspan moment in a loaded girder in two ways. If the diaphragms are torsionally stiff, they inhibit end rotation of the loaded girder at the expense of causing some end rotation in the adjacent, unloaded girders. The negative end moment so introduced in the loaded girder reduces the positive midspan moment. This behavior corresponds to a reduction in the live-load distribution factors and occurs at all skew angles.

In bridges with skew, end diaphragms also reduce the midspan moments in a second way. At the abutment, the superstructure is free to rotate about an axis parallel to the supports, but it is fixed against rotation about the axis perpendicular to the support. The end moment caused by fixity reduces the midspan moment, particularly if the skew angle is large and the end diaphragm is stiff in torsion.

The only difference between models 3 and 4 was the addition of 1.1 m thick by 2.2 m deep (42 by 85 in.) end diaphragms. For the exterior and interior girders, the addition of end diaphragms decreased the distribution factors (Fig. 12). This effect increased with increasing skew. For the exterior girders, the decrease ranged from 6% at no skew to almost 23% when the skew angle was 60°.

Effect of Continuity

The difference between models 4 and 5 was the addition of spans 1 and 3 to create a three-span, continuous bridge. The change effectively increases the longitudinal stiffness of the bridge while the transverse stiffness of the bridge remains the same. Consequently, the ratio of lateral-to-longitudinal stiffness decreases, and the load distribution factor should be expected to increase.

Fig. 13 shows the distribution factors for models 4 and 5 for a range of skew angles. For the exterior girder, distribution factors for the three-span model were higher than those of the one-span model (model 4) regardless of skew. The difference between the two models was small (<2%) at low skew angles but increased with skew (up to 15%). Zokaie et al. (1991b) also found that continuity increased the distribution factors, but a correction for this effect was not included in the AASHTO LRFD Specifications (1998).

For the interior girder, continuity decreased the live-load distribution factors for low skew angle but increased the live-load distribution factor only for skews greater than 40°. The reason for this behavior is unknown.

Effect of Skew

The ratio of distribution factor at any skew angle to the distribution factor at zero skew shows the effect of skew. Fig. 14 shows the effect of skew for the five finite-element models as well as the skew factor incorporated in the AASHTO LRFD code.

Skew had little effect for an angle of 20°, and for some models, the live-load distribution factor actually increased slightly. This finding is consistent with previous research (Bishara et al. 1993).

At larger skew angles, the live-load distribution factor decreased with increasing skew. The distribution factors in model 4 were influenced the most by skew. This result is likely due to the influence of the end diaphragms and skew discussed previously. Model 1 was least affected by skew. In general, interior girders were more affected by skew than were exterior girders. The AASHTO LRFD skew factor appears to provide

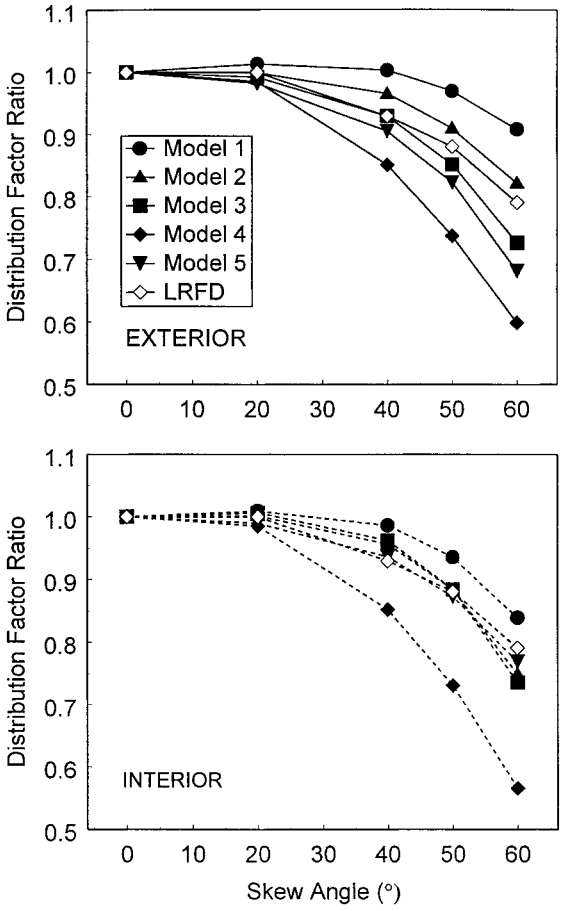

FIG. 14. Effects of Skew

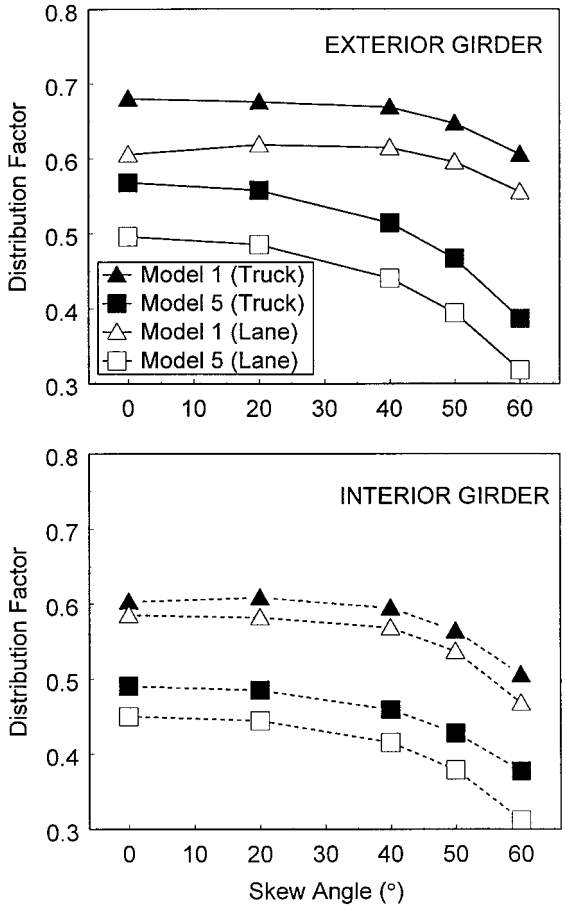

FIG. 15. Effect of Load Type

a reasonable approximation for the effect of skew in the various models.

EFFECT OF LOAD TYPE

In practice, the girder design moment from the AASHTO LRFD Specification is based on truck plus lane loading. Although the specification procedure for calculating distribution factors was developed for truck loading, it uses the same distribution factors for lane loading. Lane loading provides a significant portion of the girder design moment. According to the Washington State Department of Transportation (WSDOT) design calculations, for the SR18/SR516 overcrossing, the total midspan moment due to lane load was half of the moment due to truck load plus impact. A reduction in the lane load distribution factors could represent significant savings.

In a second series of load cases, an AASHTO distributed lane load of 9.3 kN/m (0.64 kip/ft) was applied to the lanes of each model. This uniform load was moved within each lane over a 3.0 m (10 ft) width, and nine load cases were analyzed. The application of point loads at the nodes was assumed to simulate a uniform load, because the mesh spacing was small compared with the girder spacing.

Fig. 15 shows the distribution factors for the AASHTO truck and lack loading computed using finite-element models 1 and 5. The distribution factors for lane loading are always lower than those for truck loading. On average, the lane load distribution factor is 10% lower than the truck load distribution factors. The conclusion that lane loading leads to lower distribution factors than does truck loading is consistent with the findings of Stanton (1992), who found that uniform loads are better distributed among adjacent members in precast concrete floors than are concentrated loads.

The calculated load distribution factors for truck loading were found to be lower than the ones used in the AASHTO LRFD. The calculated distribution factors for lane loading are lower still. Thus, the use of the AASHTO LRFD distribution factors to computer girder moments due to lane loading is doubly conservative for the SR18/SR516 overcrossing.

DESIGN IMPLICATIONS

The WSDOT used the LFRD code to design the bridge girders. If the distribution factors calculated with the finite-element analysis and verified by the live-load test had been used in the design of the bridge, the number of strands and the release strength could have been reduced, or the span could have been increased. To investigate this effect, the girders for the SR18/SR516 overcrossing were designed again using standard WSDOT design procedures, except that the distribution factors were obtained from the five finite-element models. All the values were calculated for bridges having a 40° skew.

Fig. 16 shows the effect of using the finite-element distribution factors on the required initial concrete strength, number of strands, and span. The final bar [model 5 (T + L)] includes separate distribution factors for truck and lane loads. The new values for release strength and number of strands were obtained while keeping the original span length. In contrast, the release strength and number of strands were kept at their original values when the new span was calculated.

If the distribution factors from model 5 (truck and lane loading) had been used to design the girders, the required release strength could have been reduced from 51 MPa (7.4 ksi) to 44.1 MPa (6.4 ksi), and four fewer strands could have been used. Alternatively, the span could have been increased by 2.1 m (6.8 ft). The reduction in release strength is particularly significant, because fabricators may have difficulty achieving the required release strength for high-performance concrete in

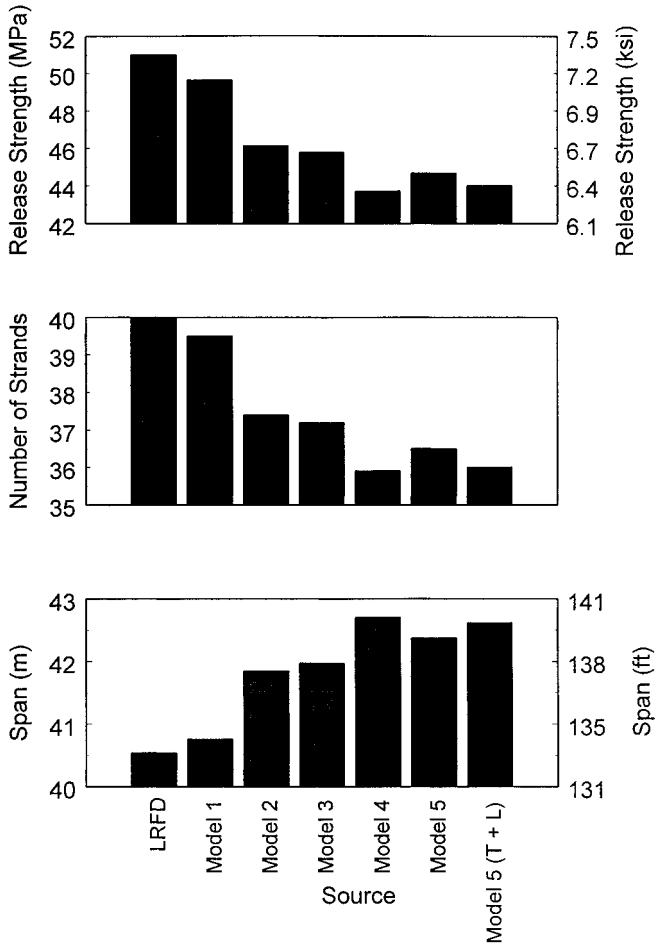

FIG. 16. Design Implications for Live-Load Distribution Factors

a 24 h cycle (Barr et al. 1998). Alternatively, the conservatism in the live-load distribution factors could be interpreted to mean that the bridge could have been designed for a 39% higher live load.

Consideration of the lift (models 1 and 2), intermediate diaphragms (models 2 and 3), end diaphragms (models 3 and 4), and lane loading [model 5 (truck) and model 5 (truck and lane)] all provided benefits. The addition of continuity (models 4 and 5) had the opposite effect. The largest changes in the design resulted from the addition of the lift and end diaphragms. Smaller changes occurred due to the addition of continuity and lane loading, while almost no change occurred when intermediate diaphragms were added.

CONCLUSIONS

A three-span, skewed prestressed concrete bridge was subjected to a live-load test and to detailed finite-element analyses. Twenty-four additional bridge configurations were analyzed to investigate the effects on live-load distribution factors of lifts, intermediate diaphragms, end diaphragms, continuity, skew angle, and load type (truck and lane). The results of these tests and analyses led to the following conclusions:

- A detailed modeling strategy of the bridge using frame elements, shell elements, and rigid constraints accurately reproduced the moments calculated from strains measured during a live-load test. The calculated maximum midspan moment for each girder was within 6% of the measured moment.
- For all 24 bridge configurations, the live-load distribution factors calculated from the AASHTO LRFD Specifications (1998) were conservative. However, the degree of conservatism varied greatly among the configurations. The distribution factors calculated with the AASHTO LRFD procedures were up to 28% larger than the factors calculated with the finite-element model that had been verified against the live-load test. In contrast, for the configuration most similar to that considered in developing the LRFD Specifications (simply supported, no lifts, no diaphragms), the code distribution factors were on average only 6% higher than those computed with finite-element analyses.
- The differences among the distribution factors from the various finite-element models were attributable to the presence of lifts, intermediate diaphragms, end diaphragms, and continuity. Adding lifts and end diaphragms significantly reduced the distribution factors. The addition of intermediate diaphragms had almost no effect on the distribution factors. Adding continuity slightly increased the distribution factors in some cases and decreased it in others.
- In all cases, the distribution factors decreased with increasing skew. This decrease was reasonably approximated by the AASHTO LRFD Specifications (AASHTO 1998).
- Distribution factors calculated for lane loading were consistently lower than those calculated for truck loading. The average decrease was 10%.
- If the distribution factors from the finite-element model of the bridge had been used to design the girders, instead of the conservative factors from the LRFD Specifications, the required release strength could have been reduced from 51 MPa (7,400 psi) to 44.1 MPa (6,400 psi). Alternatively, the bridge could have been designed for a 39% higher live load.

ACKNOWLEDGMENTS

The Washington Department of Transportation primarily supported the research presented herein. Funding for the instrumentation was provided by the Federal Highway Administration as part of a study of high-performance concrete in prestressed concrete girders. The writers would like to thank Myint Lwin, Jerry Weigel, Bijan Khaleghi, Jen-Chi Hsieh, Tom Roper, Ray Shaefer (WSDOT), and Barry Brecto (FHWA).

REFERENCES

American Association of State Highway and Transportation Officials (AASHTO). (1994a). *LRFD bridge design specifications*, 1st Ed., Washington, D.C.

American Association of State Highway and Transportation Officials (AASHTO). (1994b). *LRFD bridge design specifications*, 2nd Ed., Washington, D.C.

American Association of State Highway and Transportation Officials (AASHTO). (1996). *Standard specifications for highway bridges*, 16th Ed., Washington, D.C.

American Association of State Highway and Transportation Officials (AASHTO). (1998). *LRFD bridge design specifications*, 2nd Ed., Washington, D.C.

Barr, P. J., Fekete, E., Eberhard, M. O., Stanton,, J. F., Khalaghi, B., and Hsieh, J. C. (1998). ''High performance concrete in Washington State SR18/SR516 overcrossing: interim report of girder monitoring.'' *Rep. Prepared for the Federal Hwy. Admin.*, Washington State Department of Transportation Olympia, Wash.

Barr, P. J., Eberhard, M. O., and Stanton, J. F. (1999). *Live load distribution factors for Washington State SR18/SR516 overcrossing*, Washington State Department of Transportation, Olympia, Washington.

Bishara, A. G., Liu, M. C., and El-Ali, N. D. (1993). ''Wheel load distribution on simply supported skew I-beam composite bridges.'' *J. Struct. Engrg.*, ASCE, 119(2), 399–419.

Chen, Y., and Aswad, A. (1996). ''Stretching span capability of prestressed concrete bridges under AASHTO LRFD.'' *J. Bridge Engrg.*, ASCE, 1(3), 112–120.

Mabsout, M. E., Tarhini, K. M., Frederick, G. R., and Tayar, C. (1997). ''Finite-element analysis of steel girder highway bridges.'' *J. Bridge Engrg.*, ASCE, 2(3), 83–87.

Newmark, N. M., Siess, C. P., and Peckham, R. R. (1948). ''Studies of slab and beam highway bridges. Part I: Test of simple-span right I-beam bridges.'' *Bulletin Series No. 375*, Engrg. Experiment Station, University of Illinois, Urbana, Ill.

Nutt, R. V., Zokaie, T., and Schamber, R. A. (1987). ''Distribution of wheel loads on highway bridges.'' *NCHRP Proj. No. 12-26*, Nat. Cooperative Hwy. Res. Program, Transportation Research Board, Washington, D.C.

Ontario Ministry of Transportation and Communication (OMTC). (1992). *Ontario highway bridge design code*, 3rd Ed., Highway Engineering Division, Downsview, Canada.

SAP2000 integrated finite element analysis and design of structures. (1997). Computers and Structures Inc., Berkeley, Calif.

Sithichaikasem, S., and Gamble, W. L. (1972). ''Effect of diaphragms in bridges with prestressed concrete I-section girders.'' Civ. Engrg. Studies, Struct. Res. Series No. 383, Dept. of Civ. Engrg., University of Illinois, Urbana, Ill.

Stanton, J.F. (1992). ''Response of hollow-core slab floors to concentrated loads.'' *Prestressed Concrete Inst. J.*, 37(4), 98–113.

Stanton, J. F., and Mattock, A. H. (1986). ''Load distribution and connection design for precast stemmed multibeam bridge superstructures.'' *NCHRP Rep. 287*, National Cooperative Highway Research Program, Washington, D.C.

Westergaard, H. M. (1930). ''Computations of stresses in bridge slabs due to wheel loads.'' *Public Roads*, March, 1–23.

Zokaie, T. (2000). ''AASHTO-LRFD live load distribution specifications.'' *J. Bridge Engrg.*, ASCE, 5(2), 131–138.

Zokaie, T., Osterkamp, T. A., and Imbsen, R. A. (1991a). ''Distribution of wheel loads on highway bridges.'' *Transp. Res. Rec. 1290*, Transportation Research Board, Washington, D.C.

Zokaie, T., Osterkamp, T. A., and Imbsen, R. A. (1991b). ''Distribution of Wheel Loads on Highway Bridges.'' *NCHRP Proj. Rep. 12-26*, Transportation Research Board, Washington, D.C.